

# Introducing the Post-Glacial Land Adjustment Regenerator (GLARE) for simulating the Final Pleistocene/Holocene geographic change in North Europe



Aki Hakonen<sup>ID</sup>

Archaeology, University of Oulu, Finland

## ARTICLE INFO

### Keywords:

Post-glacial  
Glacial isostatic adjustment  
Simulation  
Holocene  
Final Pleistocene  
North Europe  
Landscape archaeology  
QGIS

## ABSTRACT

Glacial isostatic adjustment produces challenges and opportunities for northern archaeology. Landscapes, coastlines, and lake shores have undergone continual change due to sea-level rise, land uplift, tilting, and water drainage. Simulating the combined effect brings to life a veritable geographic clockwork, which frames human habitation. In landscape archaeology the effect has usually been modelled on the basis of incommensurable local uplift/sea-level curves. This paper presents a new general semi-empirical land uplift model for digital terrain model morphing that is applicable throughout North Europe within the former extent of the Fennoscandian Ice Sheet. The first refined version of the model is designed for open access use in QGIS software. Based on validation testing on 1542 index points, the model functions on par with earlier complex models, albeit with better accessibility. The GLARE model provides a generalized method for simulating geographical change in North Europe, providing new possibilities for landscape archaeology.

## 1. Introduction

The land throughout North Europe is rising imperceptibly but measurably (e.g. Lidberg et al., 2010; Lahtinen et al., 2022). This effect, glacial isostatic adjustment (GIA), is caused foremost by local Late Pleistocene glacial history (see e.g. Tikkainen and Oksanen, 2002; Lunkka et al., 2004; Lundqvist, 2004; Steffen and Wu, 2011; Stroeven et al., 2016; Patton et al., 2017). Between 30,000 and 10,000 years ago massive sheets of ice dominated the surface geography of the north, reforming superficial deposits and depressing the land underneath. After the Final Pleistocene and Early Holocene climate warming, glacial retreat caused the land to rebound. Meanwhile, sea-levels around the globe reacted to the warming climate and glacial melting, causing waters to rise (Smith et al., 2011), which, in conjunction with the regional land uplift powered by the loss of glacial mass, resulted in a continual redrawing of coastlines.

In its heyday in ca. 19 kya the Fennoscandian Ice Sheet (FIS) reached Southern Jutland, Central Europe south of the Baltic Sea, and Northwest Russia (Fig. 1; Patton et al., 2017; Sejrup et al., 2022). The glacial mass covered modern-day Finland, Estonia, Sweden, and Norway, coalescing with the smaller British-Irish Ice Sheet (BIIS) in the southwest and the Barents-Kara Ice Sheet to the northeast (Hughes et al., 2014; Patton

et al., 2016). The maximum thickness of FIS is estimated at 2.7 km (Patton et al., 2017). During its 9000-year melt, until c. 8000 BCE, the outer extremes of FIS slowly retracted to its final vestige in the highlands of Norrland (where the arrows converge in Fig. 1; Lundqvist, 2004; Lindén, 2006; Patton et al., 2017). Throughout the former domains of ice sheets varying rates of glacial isostatic adjustment remains in effect.

Understanding land uplift is one of the major components in northern archaeology (see e.g. Siiriläinen, 1978; Jussila, 2000; Bergman et al., 2003; Okkonen, 2003; Seitsonen, 2005; Vaneckhout, 2009, 2012; Herva and Ylimaunu, 2014; Hakonen, 2017; Tallavaara and Pesonen, 2020; Manninen et al., 2021; Skantsi et al., 2023). Though the effect remains a fraction of what it was at its onset, within just the last 500 years several historical towns in the northern Baltic Sea have become separated from the shore, hindering maritime trade (Ekman, 2009: 21–9). Due to the same effect, Mesolithic and Neolithic coastal dwelling sites in Finland are commonly found far inland (e.g. Vaneckhout et al., 2012; Bracewell, 2020; Hakonen, 2021; Skantsi et al., 2023). Furthermore, accurate knowledge of future uplift—deriving from past trajectories—in relation to sea-level rise is of great importance in zoning and urban planning as well as hi-tech industrial development, such as the planning of offshore wind farms and nuclear power plants (e.g. Ikonen and Helin, 2011).

E-mail address: [aki.hakonen@oulu.fi](mailto:aki.hakonen@oulu.fi).

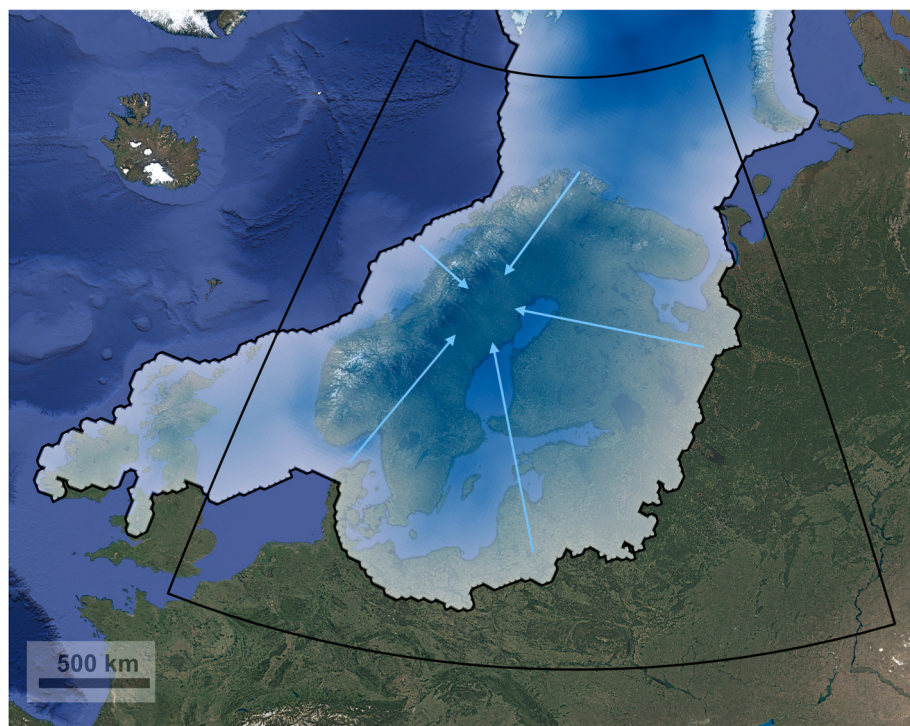


**Fig. 1.** The maximum extent of the North European glaciation at ~17000 BCE and the ~9000-year retreat of FIS. Rounded trapezoid indicates the current region of application for the GLARE model. Glacial model by Henry Patton (in Sejrup et al., 2022). Background Google Satellite.

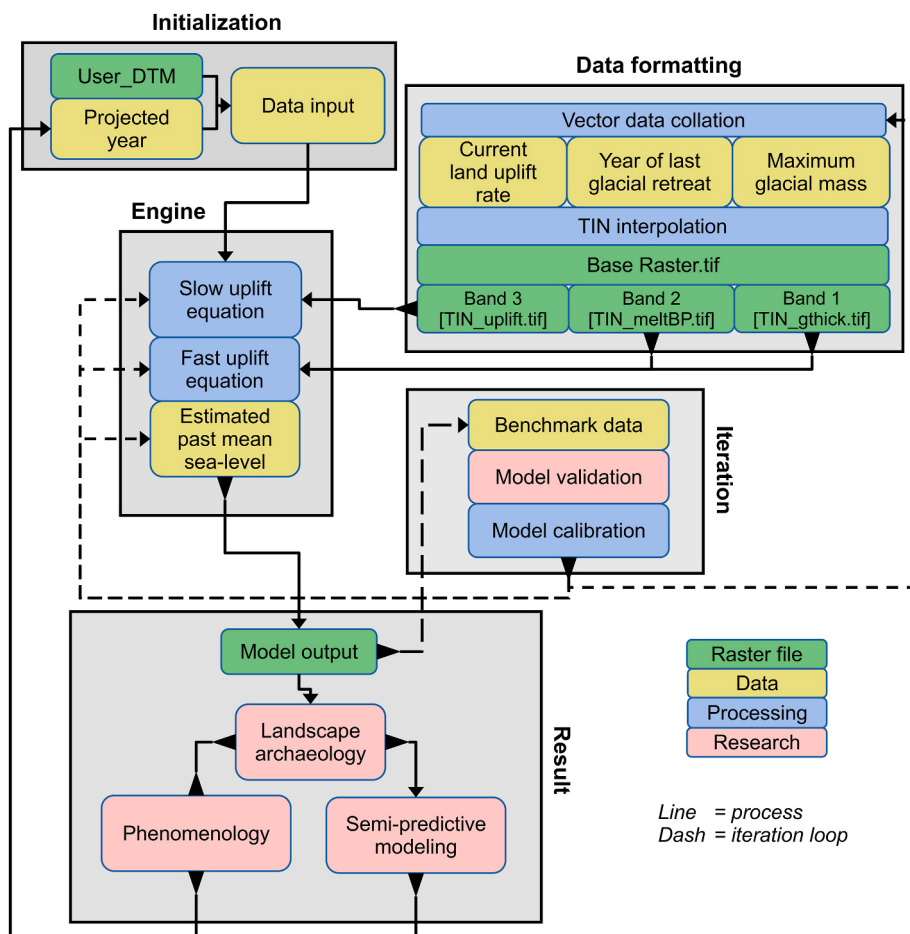


**Fig. 2.** Model pipeline from initialization and data formatting to running the engine and applying the output in research. Note the iteration loop.

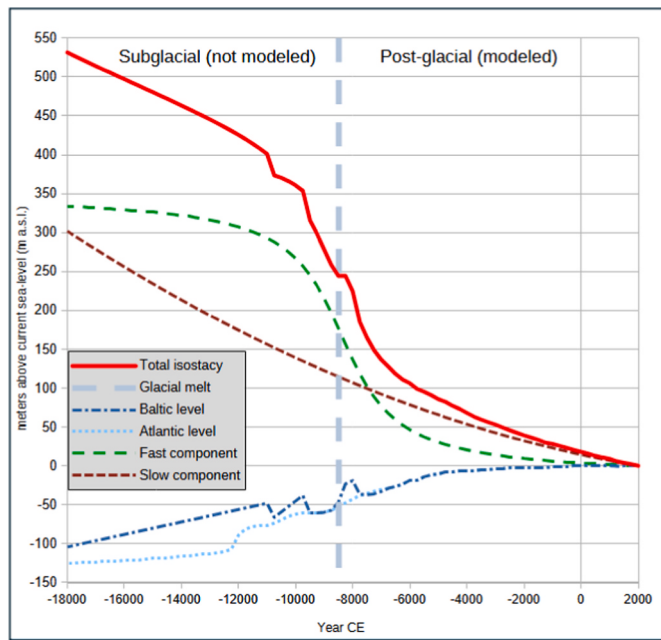


**Fig. 3.** Fast component + slow component - sea-level component = simulated elevation. Example from Central Fennoscandia, from where the glacier retreated at around 8500 BCE.

Despite major advances of the field, there are two main problems in the archaeological application of isostacy modelling: (1) the most advanced models can be too convoluted to apply in practice by non-specialists; (2) the commonly applied models function regionally case-by-case, based on local sea-level/land uplift curves or lake-tilt gradients, and are difficult to apply outside the predefined regional scopes.

This paper presents a new generalized method for simulating land uplift in Fennoscandia and the Baltic region, with emphasis on accessibility, usability, wide applicability, and ease of validation and correction. The Post-Glacial Land Adjustment Regenerator (GLARE) model is developed for QGIS (a free and open-source geographic information system) where it functions by mathematically recalculating current digital terrain model (DTM) cells to simulate past geography (Fig. 2). The model addresses inherent flaws in earlier methods of landscape reconstruction commonly used in archaeology.

## 2. Method

The simple formula for the model is *fast component + slow component + sea-level component*. The method was developed by geologist Tore P  sse (2001). The method aims for best fit in relation to sea-level index points (SLIPs). The approach was criticized by Kurt Lambeck (2006) for its disregard of actual physics but has remained in use (e.g. Vuorela et al., 2009). While the method does not represent the physics of glacial isostatic adjustment, it does simulate the effects efficiently and with ease of access and is applicable in DTM recalculation. The purpose of this model is to provide both accessibility and accuracy for landscape archaeological and geographic research. The slow component extrapolates the current measured land uplift, applying a deceleration factor over time, while the fast component represents the accelerated uplift rate and its rapid deceleration in the few millennia after deglaciation. The fast component applies an arctangent function (P  sse and Andersson, 2005), which produces a symmetrical slanted S-shaped curve (hyperbolic tangent) on the XY-plot (Fig. 3). The steepest gradient in the centre of the S simulates the fastest uplift and is synchronized to localized raster values (*TIN\_meltBP.tif*) that define the year of glacial retreat, i.e. when the land became free from the depressing force. The maximum thickness of the glacier in ca. 19–22 kya (Patton et al., 2016, 2017;

**Table 1**

List of variables and parameters for formula.

Variable	Description	Value/Source	Classification
y	Year in CE	User-defined <sup>a</sup>	Custom
z	Elevation in m	User DTM	Custom
h	Max. thickness of ice in m	<i>TIN_gthick.tif</i>	Semi-empirical
r	Year of glacial retreat	<i>TIN_meltBP.tif</i>	Semi-empirical
v	Current uplift velocity, mm/year	<i>TIN_uplift.tif</i>	Semi-empirical
s	Mean sea-level	Sea-level reference card <sup>a</sup>	Semi-empirical
t	Year of DTM	[2020] <sup>b</sup>	Custom
a	Variable 1 for fast component	5	Abstract
b	Variable 2 for fast component	500	Abstract
C <sub>h</sub>	Calibration of h to mass factor	0.075	Abstract
C <sub>v</sub>	Calibration factor for v	0.072	Abstract
d	Deceleration factor for v	0.014	Abstract

<sup>a</sup> manually applied.

<sup>b</sup> marginal value representing the measurement year of User DTM.

Sejrup et al., 2022) is applied as the raster value (*TIN\_gthick.tif*) determining the local depressing force.

The slow component is based on a formula by geologist Marjatta Okko (1967), and was further calibrated by Okkonen (2003) and Hakonen (2017). This formula is applied since it is anchored on empirical current isostatic uplift rates and it has previously tested well against archaeological sea-level index points. The slow component compounds the current GNSS (Global Navigation Satellite System) measured isostatic land uplift—*TIN\_uplift.tif*, based on NKG2016LU (Vest  l et al., 2019)—with time, amending the resulting linear growth with a marginally exponential deceleration factor (Fig. 3). Extrapolating to the past from the present day thus provides faster uplift in the past, which slows down as time progresses. Due to the added effect of the fast component, both components are further calibrated to account for their combined effect.

The sea-level adjustment simulates the mean Oceanic (Atlantic) and Baltic Sea (inland lake) levels (Fig. 3). These are semi-empirical datasets of observed relative sea-level rise at near-null-uplift regions drawn from published data from both sides of the Southeast Denmark threshold that separates the Atlantic mean (Spratt and Lisiecki, 2016; Mejles et al., 2018; J  ns et al., 2020; Stattegger and Leszczy  ska, 2023) from the Baltic mean (U  cinowicz, 2004; Bennike and Jensen, 2013; Nilsson et al., 2020; Lampe and Lampe, 2021;   uklus and Girinkas, 2022). The sea-level components are identical except during periods when the Baltic Sea was isolated from the sea (i.e. Baltic Ice Lake, c. 14,000–9650 BCE, and Ancylus Lake, c. 8700–6500 BCE). Both datasets follow trends determined in prior research, but the sea-level elevations are calibrated to fit the model, and thus they are semi-empirical. The sea-level adjustment is applied separately, making it the non-computational weak link of the model (see Borreggine et al., 2022), but it allows easy regional adjustment in accordance with local observations.

There are total 12 variables in the applied formula (Table 1). Two—year (y) and elevation (z)—are case-specific and user-defined. Five are free-floating abstract values which relate to the inner mechanics of the formula. Four are evidence-based semi-empirical values, adjustable within their published or interpreted error margins. The four variables are 1. maximum thickness of glacial ice h (in meters), 2. year of the glacial retreat r (in calBP), 3. current measured land-uplift v (in mm/year), and 4. eustatic sea-level s (in meters above current zero elevation). The first three are represented by GeoTIFF-files that in the online material are merged into bands 1–3 of the *Base Raster.tif* file (Fig. 4).

The sea-levels are represented by two graphs, oceanic and Baltic. The Baltic sea-level data should be applied when the User DTM uses the

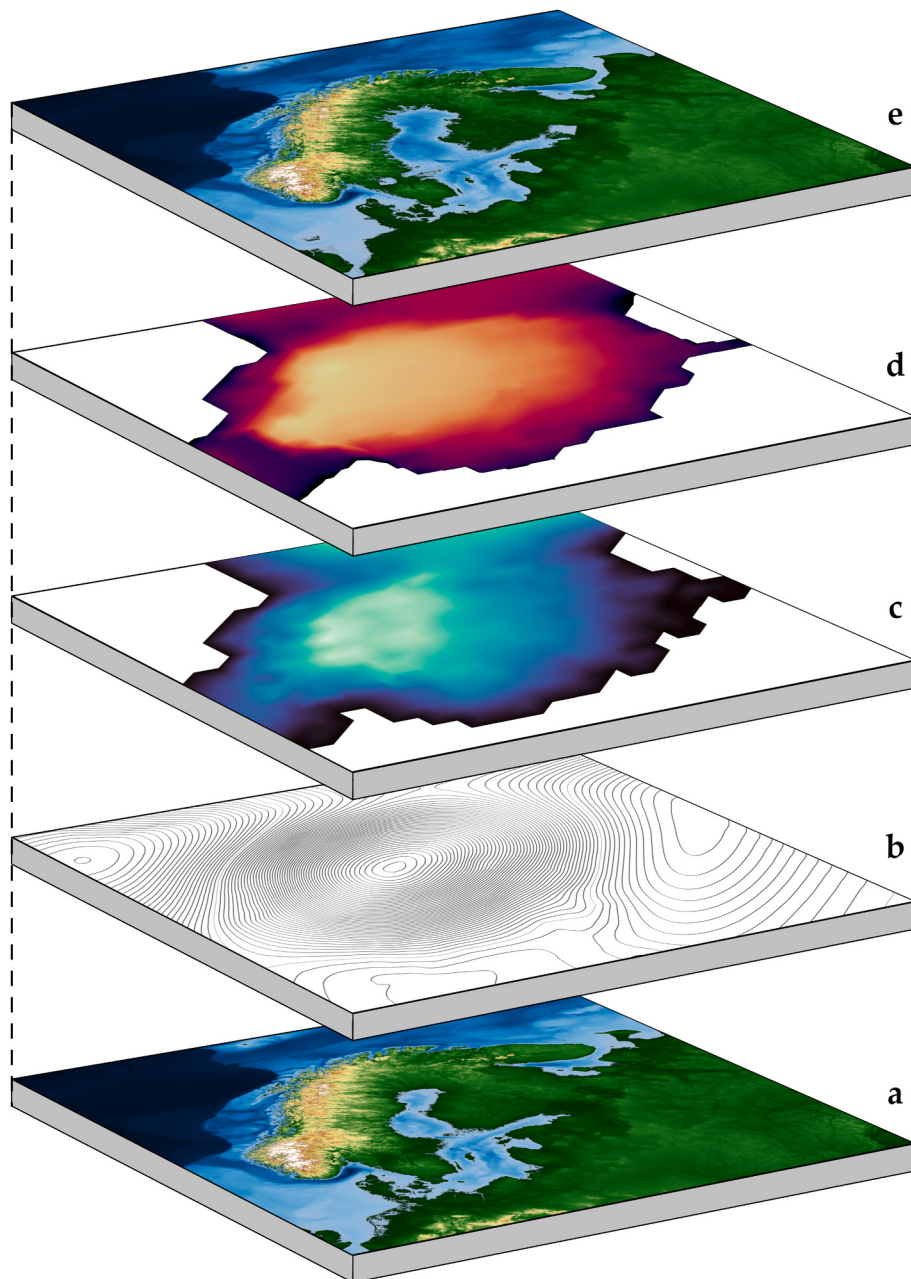


**Fig. 4.** DTM reconstruction for 6000 BCE. The original hydrographic model GEBCO 2024 (a) at the bottom applied with TIN\_uplift.tif (b), TIN\_gthick.tif (c) and TIN\_meltBP.tif (d) results in the reconstruction (e) on top.

Baltic level as the zero elevation point and the simulated timeframe overlaps with the two inland lakes, the Baltic Ice Lake and Ancylus Lake. In cases where both the oceanic and the Baltic levels are pertinent, the Baltic lakes are best simulated by either cropping a Baltic zone from the related DTM and applying the Baltic level on to it, or by drawing a contour to represent the Baltic lakeshore.

The model does not simulate the accumulation of sediment or the effects of modern land use (see e.g. [Habicht et al., 2017](#)) in DTM recalculation, nor gravitational or rotational effects (e.g. [Bamber and Riva, 2010](#)) of ice sheets. Such effects should be considered and modelled locally wherever they apply. The equation reads as follows (for QGIS syntax see [Supplement](#)):

$$Z_y = z - \left( \frac{2}{\pi} (hC_h) \arctan \left[ \left( \frac{r}{a(hC_h) + b} \right) - \arctan \left( \frac{r \cdot y}{a(hC_h) + b} \right) \right] \right) + \left( \left[ (vC_v) \frac{t \cdot y}{100} \right] - \left[ 0.5 \times -d(vC_v) \left( \frac{t \cdot y}{100} \right)^2 \right] \right) - s_y$$

In addition to manual application, an automated GLARE-model—compiled with QGIS Model Builder—is applicable via QGIS Toolbox (<https://doi.org/10.5281/zenodo.15772211>). It is loaded by applying Add Model to Toolbox on *GLARE.model3* and loading *Base Raster.tif* and either *sea-level-oceanic.tif* or *sea-level-baltic.tif*.

### 3. Validation and results

There are several conditions which the model should predict in order to be deemed properly functioning. Ideally, the model should come as close as possible to fitting the highest shorelines ascertained from the

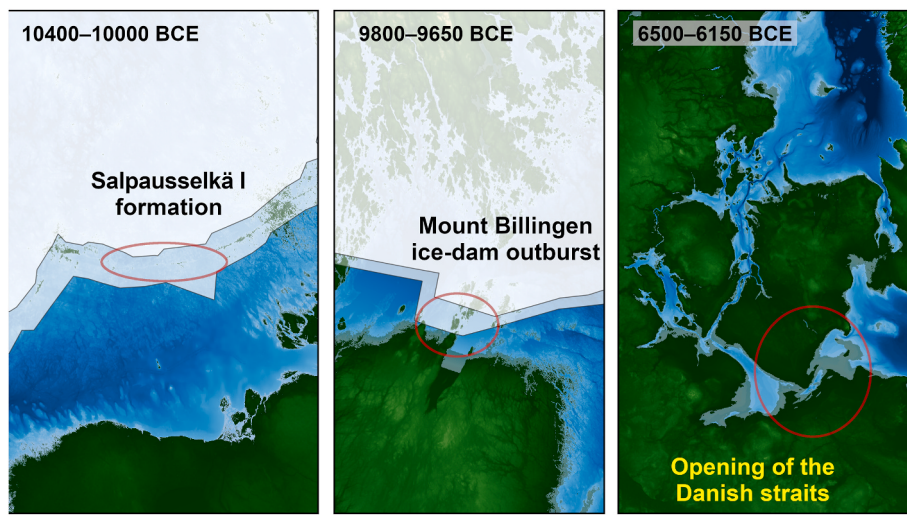


**Fig. 5.** First validation: Three benchmark panels simulating the retreat of the glacial sheet and the emergence land (left and middle panels), and marine transgression (right panel). Simulation made with GEBCO 2024 15 arc-second hydrographic model.

geological records of Finland and Sweden (Ojala et al., 2013; Pässe and Daniels, 2015). These benchmarks will not be applied here since they are not absolutely dated and are often interpretative (but see Supplement, '94 – High coast test'). Instead, in the first validation the model should match the three following sufficiently well-dated geographic events that had long-term consequences for the Baltic Sea history (see e.g. Lambeck, 1999): Salpausselkä I glacial standstill of 10200–10300 BCE in Southern Finland during the Baltic Ice Lake phase (Donner, 2010; Lunkka, 2023), Mount Billingen outburst of 9650–9700 BCE in Central Sweden marking the beginning of the Yoldia Sea (Lambeck, 1999; Andrén et al., 2002; Jakobsson et al., 2007; Öhring et al., 2020; Lunkka, 2023) and the opening of the Danish straits between 6000 and 6500 BCE marking the

shift from the Ancylus Lake to the Littorina Sea (Lambeck, 1999; Lemke et al., 2002; Björck et al., 2008; Bennike et al., 2012, 2021). Since the first two are dictated largely by the specifically synced glacial retreat raster values, the test result rests mostly on the independent Danish straits event. The acceptable error margin for the first three geographic tests in this iteration is set at  $\pm 200$  years.

The model simulates the three events as occurring in 10400–10000 BCE (Salpausselkä I), 9800–9650 BCE (Mount Billingen outburst) and 6500–6150 BCE (opening of the Danish straits) (see Fig. 5), placing them within the margin. For now though, the glacial retreat raster dataset does not represent the glacial standstills accurately as the retreat merely decelerates instead of halting. Simulating glacial standstills, where the

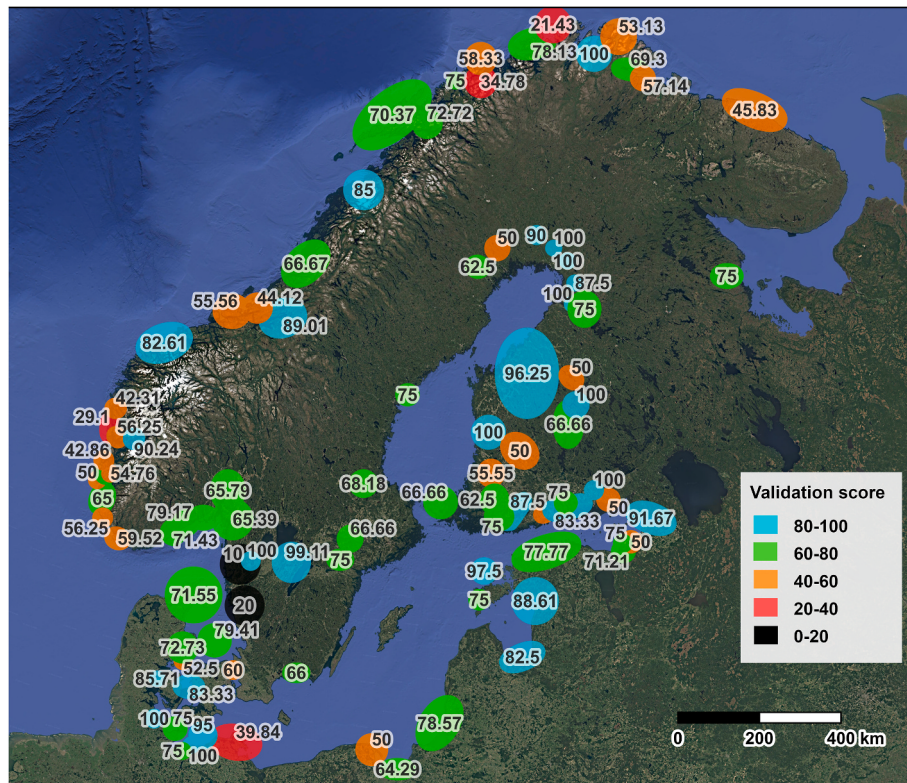


**Fig. 6.** Validation scores (%) per zone. Localized uplift curves and the sea-level index point data are available in the online supplement. Background Google Satellite.

**Table 2**

Second validation test results compared with prior models (# per zones).

Zonal quality	Synced	Functional	Limited	Erroneous	Unsynced
Validation score	80–100 %	60–80 %	40–60 %	20–40 %	0–20 %
<i>GLARE (this paper)</i>					
Frequency	33	37	17	6	3
Representation	34.38 %	38.54 %	17.71 %	6.25 %	3.13 %
Average validation score: 70.14 %					
<i>STEHME (in Creel et al. 2022)</i>					
Frequency	12	18	2		
Representation	37.50 %	56.25 %	6.25 %		
Average validation score: 77.14 %					
<i>ICE-5G/ICE-6G_C (in Rosentau et al. 2021)</i>					
Frequency	12	7	4	7	10
Representation	30.00 %	17.50 %	10.00 %	17.50 %	25.00 %
Average validation score: 50.42 %					
<i>Hyperbolic tangent (in Vuorela et al. 2009)</i>					
Frequency	3	6	4		
Representation	23.08 %	46.15 %	30.77 %		
Average validation score: 72.47 %					

glacial retreat stopped to form high moraine ridges, will require more fine-tuning.

The second test is to compare regional uplift curves to a selection of 1636 sea-level index points provided by Rosentau et al. (2021) and Creel et al. (2022), as well as additional sources (Vuorela et al., 2009; Ojala et al., 2013; Skantsi et al., 2023). These SLIPs include mostly radiocarbon dated—and to a lesser extent interpreted—submarine, coastal, and terrestrial contexts. It should be noted that especially radiocarbon dated submarine contexts may involve further uncertainties additional to the statistical radiocarbon error margins due to the unpredictable circulation of carbon isotopes underwater, including the reservoir effect (see e.g. Bennike et al., 2012; Quarta et al., 2021; Hadden et al., 2023). Conflicting dates should ideally be considered based on their contextual data, but with a large dataset to compare, such detail has to be set outside the scope of the test. Arguably, archaeological AMS-dated terrestrial limiting points should be considered most reliable, since the dated materials vary and there is less chance that they are affected by systematic errors, and the dated contexts are by default *in situ*.

Note that the uncertainty factor in SLIP elevations has not been considered here. A Gaussian distribution for SLIP elevation uncertainties is expected, with the reported median the most probable elevation. The elevation uncertainties of each SLIP is listed in the supplemental material for case-by-case consideration.

The larger SLIP dataset is tested with a binary TRUE/FALSE validation statement for each index point from 96 benchmark zones (Fig. 6; also *Supplemental Map*). The zones were drawn based on the clustering of datapoints. To merit validation 1 (or TRUE), a terrestrial limiting point should reside above the simulated shoreline curve, a marine limiting point below it, and a mean-sea-level point along the curve within a 2-sigma temporal probability margin. An archaeological point should be minimum 1.5 m above the water-level curve. For this test a total 50 % validation score would be operational yet limited while a 60 %+ score would be functional, as it would have similar validation to related models (Table 2). Due to inaccuracies and perceived contradictions within the SLIP dataset the maximum expected validation score is 80 %.

The SLIP database validation score for the model is 70.14 % overall indicating a functional model. This is the average of the mean validation score from the 96 zones (Fig. 6). Each datapoint was evaluated as 1 (TRUE) or 0 (FALSE) depending on whether the model predicted its depositional context as either above, below or near mean sea-level. The total number of compared datapoints is 1542 (with 85 datapoints additional to Rosentau et al., 2021; Creel et al., 2022 and 94 discarded

for being either too obvious or clearly erroneous, see *Supplement*). The validation scores of the zones were averaged so that each zone is weighed the same. As individual markers the data points validate at 1071 out of 1537, or total score 69.68 %.

The most indicatively erroneous regions are in Västra Götaland in Sweden, the Pomeranian coast of Germany, and various locales near Bergen and Troms in Norway. The validation of Västra Götaland consists mere eight samples published in 1969 and 1973 (see *Supplement*, Zones 43–4) so newer SLIPs should be compared before any adjustments. Inconsistencies near Bergen and Troms can be easily explained by ice margin behaviour, on which basis the ice model can be calibrated in the future. The Pomeranian coast (Zone 29) contains a series of 50 mean sea-level indicator points from 1500 CE to 7000 BCE (see Lampe et al., 2010) to which the uplift curve is ~14 % out of sync, although the possibility of systematic errors in the peat bulk dates should be investigated (e.g. Hedenstrom and Possnert, 2001) before forcing a correction.

Still, the validation of the zones overall either outperforms or performs on par (Table 2) with prior ICE-5G, ICE-6G and GLAC-1D models tested by Rosentau (et al., 2021) and (Creel et al., 2022). In the future these zones and more can be further calibrated to more accurate sea-level index points by fine-tuning the variables and modifying the underlying raster datasets, especially by refining current land uplift rates within their observed error margins and adjusting the year when the ice sheet melted.

## 4. Discussion

### 4.1. Flaws and adjustments

While GLARE already functions on par with similar models, it has its flaws.

- a.) The synchronization to the SLIPs is not yet fully optimal, but can be refined in later versions. More testing with archaeological index points that conclusively date activity on the coastline (see e.g. Bennike et al., 2023) is needed. Such archaeological dates are more accurate and less error prone than geological dates from marine and lacustrine deposits, which even when AMS dating provides narrow apparent error margins may in actuality contain much wider uncertainty factors, as evidence by multiple inconsistencies within the applied SLIP dataset.
- b.) Also, the formula used by GLARE is not optimized for efficiency, as it carries over calibration factors resulting from the merging of two different formulae. This reduces the processing efficiency, which due to the multiplication of the calculation when applied on raster cells—regularly millions or even billions—may significantly increase processing time. With large datasets the optimization of the formula could yield significant efficiency benefits.
- c.) The largest abstraction in GLARE is the sea-level adjustment. Borreggine et al. (2022) have argued that sea-level should in such models be regarded as contextually dynamic and mathematically solvable based on the gravity of mass. In the future a more nuanced sea-level model should be tested. Currently the abstract water level should always be regarded as dynamic and annually as well as diurnally fluctuating, dependent on weather and season, but modelling short-term effects in detail is usually only manageable at a very local scale. In cases where the model erroneously places a set of dating samples below mean water level, such evidence should act as a Bayesian benchmark, which should foremost be corrected by adjusting the abstracted sea-level.
- d.) A major flaw in the current model is that the GNSS measurement data is not spatially systematic. Russia on the whole is deficient in relative refined data, and many regions throughout Finland also contain blind spots, while the Baltic and Scandinavia are better represented. The relative uplift between regions will need further

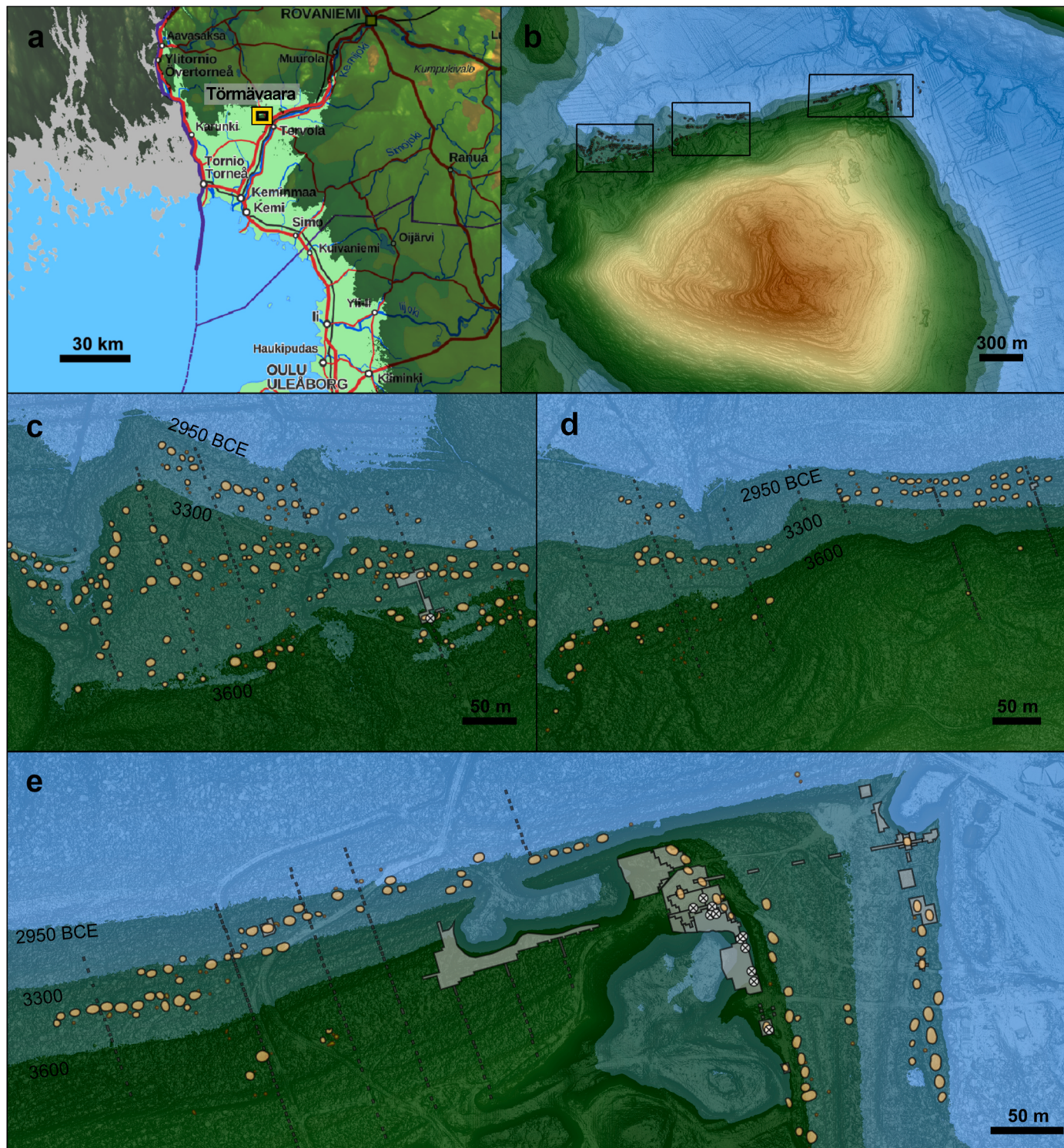


**Fig. 7.** Törmävaara Neolithic dwelling site, consisting of 300 shallow depressions made by semi-subterranean dwellings. Simulated shorelines from 2950 to 3600 BCE highlighted, at 53–62 m above current sea-level. Lidar data by National Land Survey of Finland.

testing and calibration as it is expected that more GNSS data will become available in time (a next generation dataset to NKG2016LU was made available by Lahtinen et al., 2022). As the error margin compounds in time, and the correct declination of the initial fast uplift gradient immediately after glacial retreat is difficult to determine, the most error prone context is the first two millennia after deglaciation. However, the model is adequately

reliable in most regions of North Europe during the last ten millennia to be further trialled in practice.

#### 4.2. Merits and application

The model does have significant merits.

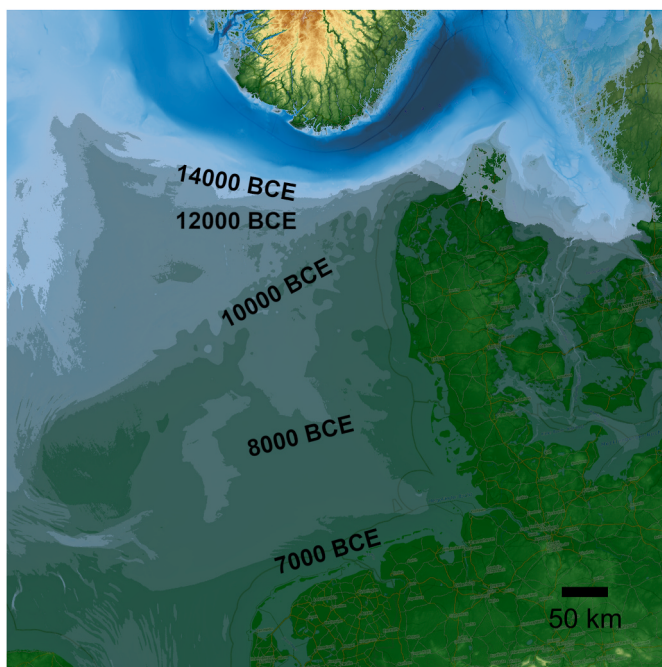


**Fig. 8.** Doggerland simulation 7000–14000 BCE with shaded coastlines west of Denmark. Modified GEBCO\_2024 Bathymetry. Background OpenTopoMap.

a.) GLARE allows access to land/lake tilting in combination with coastal shoreline displacement. Lake tilt can be modelled by running GLARE and determining the likeliest simulated elevation of the contemporary lake outflow and running Contour Polygon according to the specified elevation (applying  $-fl z$  expression). These outflows have often changed in time as lake tilting may have resulted in a prior outflow's elevation ascending relative to the lake's central axis, forcing a new primary outflow at a descended shore. All lakes have unique histories, which can be

accessed either through prior geological, geographical or historical research (e.g. Hakulinen, 2024), or by spatially examining the relative elevations of fossilized outflows and terraces recorded in the landscape. Accurate modelling of lake tilting usually requires underwater hydrological depth data to combine with the used DTM, although simple approximations can be made without it.

- b.) Although the model can be applied to the future to see the combined effect of land-uplift and sea-level change, it is designed mainly for extrapolation into the past. It can be applied, especially in contexts of continuous relative sea-level regression, to cost-effectively date the landscape phases of sites. This technique has proven particularly useful in dating Neolithic forager dwelling sites where houses are marked by depressions in the terrain that are distinguishable in lidar. Such houses are assumed to be primarily connected with shorelines (see Fig. 7; e.g. Tallavaara and Pesonen, 2020; Hakonen, 2021; Skantsi et al., 2023). This shoreline displacement chronology, which establishes terminus post quem dates, can be applied to large datasets to establish the dynamics of long-term change in the archaeological record.
- c.) Furthermore GLARE makes landscape change more accessible, since its practical temporal scale is a single year. Thus, even local year-by-year or decade-by-decade change can be assessed. This adaptability opens up new opportunities for the phenomenological study of animate landscapes. The perception of the landscape being alive is likely to have had profound cosmological implications (see e.g. Herva and Ylimaunu, 2014; Herva and Lahelma, 2020).
- d.) GLARE is applicable for further maritime hydrological study, either in the Southern Baltic (e.g. Žulkus and Girininkas, 2022) or the Doggerland region (Fig. 8; see e.g. Pieters et al., 2020; Bailey and Cawthra, 2023), providing new opportunities for the discovery of underwater archaeological sites. Despite its inaccuracies, particularly during the first two millennia after deglaciation, the model is still pertinent in the study of the Final Palaeolithic and Mesolithic, when the North European landscapes were undergoing extreme animate change (Fig. 9). GLARE can be used as

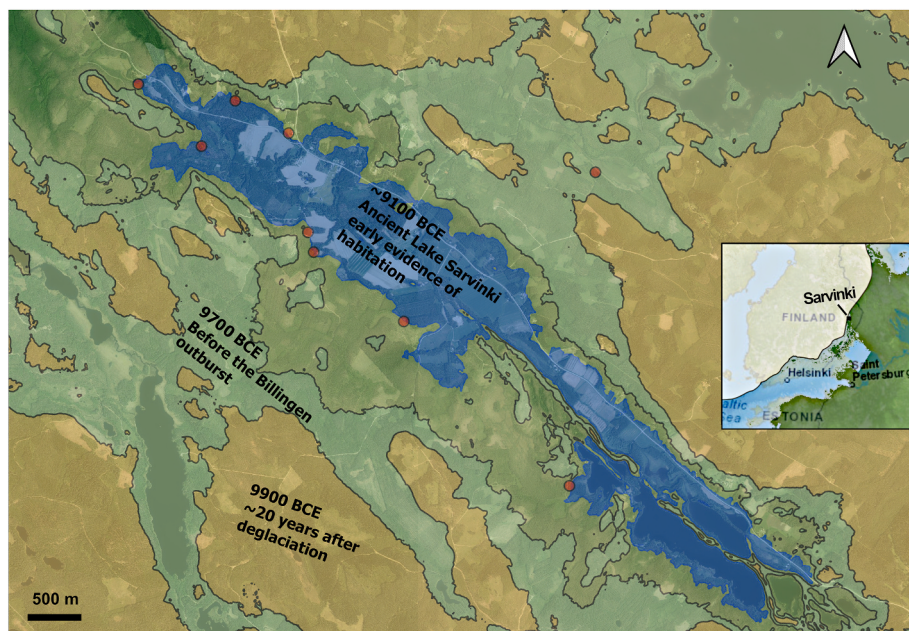


**Fig. 9.** Changing coastlines of the Early Mesolithic in Eastern Finland according to GLARE. Red dots are prehistoric dwelling sites (see Pesonen et al., 2022). By 9100 BCE the coastline had advanced to the west, leaving the lake far inland. Minimap shows the location of Lake Sarvinki with FIS and GLARE reconstruction at 9900 BCE based on GEBCO\_2024. Background Orthophoto by the National Land Survey of Finland. (For interpretation of the references to colour in this figure legend, the reader is referred to the Web version of this article.)

a veritable world-builder in these contexts whose archaeological records are by themselves extremely elusive relative to later time periods.

## 5. Conclusions

GLARE provides an accessible general-purpose model for studying Holocene and Final Pleistocene land uplift and sea-level change in North Europe. More usage and critical assessment are needed to refine the model based on local benchmarks. However, even in its current form, the model competes well with prior models due to increased availability of benchmark data, according to which the current iteration is calibrated. While future improvements may increase usability, GLARE already provides easy access to the reconstruction of animate landscapes. The method opens up new possibilities and a novel grounded method especially for the archaeological study of the Final Palaeolithic and Mesolithic Age, the material evidence of which are otherwise notoriously elusive in Northern Europe.

## Online data

GLARE latest build: [https://github.com/Hakonaki/land-uplift-reco\\_n](https://github.com/Hakonaki/land-uplift-reco_n)

GLARE archived version (2.2): <https://doi.org/10.5281/zenodo.1572211>

## Funding statement

This study received no funding.

## Declaration of competing interest

The authors declare that they have no known competing financial interests or personal relationships that could have appeared to influence the work reported in this paper.

## Acknowledgments

The model was inspired by early testing made by Janne Ikäheimo of the University of Oulu. Glaciologist Henry Patton of UiT courteously provided a workable glacial model, and archaeologist Marianne Skandfer of UiT provided initial archaeological index points for Northeast Norway. Special thanks to Karen Niskanen for asking difficult questions with difficult answers.

## Appendix A. Supplementary data

Supplementary data to this article can be found online at <https://doi.org/10.1016/j.jas.2025.106298>.

## References

- Andrén, T., Lindeberg, G., Andrén, E., 2002. Evidence of the final drainage of the Baltic Ice Lake and the brackish phase of the Yoldia Sea in glacial varves from the Baltic Sea. *Boreas* 31, 226–238. <https://doi.org/10.1111/j.1502-3885.2002.tb01069.x>.
- Bailey, G., Cawthra, H.C., 2023. The significance of sea-level change and ancient submerged landscapes in human dispersal and development: a geoarchaeological perspective. *Oceanologia* 65 (1), 50–70. <https://doi.org/10.1016/j.oceano.2021.10.002>.
- Bamber, J., Riva, R., 2010. The sea level fingerprint of recent ice mass fluxes. *Cryosphere* 4, 621–627. <https://doi.org/10.5194/tc-4-621-2010>.
- Bennike, O., Jensen, J.B., 2013. A Baltic Ice Lake lowstand of latest allerød age in the Arkona Basin, southern Baltic Sea. *GEUS Bulletin* 28, 17–20. <https://doi.org/10.34194/geusb.v28.4710>.
- Bennike, O., Andreassen, M.S., Jensen, J.B., Moros, M., Noe-Nygaard, N., 2012. Early Holocene sea-level changes in Øresund, southern Scandinavia. *GEUS Bulletin* 26, 29–32. <https://doi.org/10.34194/geusb.v26.4744>.
- Bennike, O. J. B., Jensen, Nørgaard-Pedersen, N., Andreassen, K.J., Seidenkrantz, M.-S., Moros, M., Wagner, B., 2021. When were the straits between the Baltic Sea and the Kattegat inundated by the sea during the Holocene? *Boreas* 50, 1079–1094. <https://doi.org/10.1111/bor.12525>.
- Bennike, O., Philipsen, B., Groß, D., Jessen, C., 2023. Holocene shore-level changes, southern Lolland and the Femern Belt, Denmark. *J. Quat. Sci.* 38 (3), 440–451.
- Bergman, I., Pässe, T., Olofsson, A., Zackrisson, O., Hörnberg, G., Hellberg, E., Bohlin, E., 2003. Isostatic land uplift and Mesolithic landscapes: lake-tilting, a key to the discovery of Mesolithic sites in the interior of Northern Sweden. *J. Archaeol. Sci.* 30, 1451–1458.
- Björck, S., Andrén, T., Jensen, J.B., 2008. An Attempt to Resolve the Partly Conflicting Data and Ideas on the *Ancylus-Littorina* Transition, 23. Polish Geological Institute Special Papers, pp. 21–26.
- Borreggine, M., Powell, E., Pico, T., Mitrovica, J.X., Meadow, R., Tryon, C., 2022. Not a bathtub: a consideration of sea-level physics for archaeological models of human migration. *J. Archaeol. Sci.* 137, 105507. <https://doi.org/10.1016/j.jas.2021.105507>.
- Bracewell, J., 2020. Monuments, Territories and Post-sedentism Among the Pre-historic hunter-gatherers of Coastal Northern Finland. McGill University, Montreal. *PhD dissertation*.
- Creel, R.C., Austermann, J., Khan, N.S., D'Andrea, W.J., Balascio, N., Dyer, B., Ashe, E., Menke, W., 2022. Postglacial relative sea level change in Norway. *Quat. Sci. Rev.* 282, 107422. <https://doi.org/10.1016/j.quascirev.2022.107422>.
- Donner, J., 2010. The Younger Dryas age of the Salpausselkä moraines in Finland. *Bull. Geol. Soc. Finland* 82, 69–80. <https://doi.org/10.17741/bgsf/82.2.001>.
- Ekman, M., 2009. The changing level of the Baltic Sea during 300 years: a clue to understanding the Earth. Godby: Summer Institute for Historical Geophysics Åland Islands.
- Habicht, H.-L., Rosentau, A., Jöeleht, A., Heinsalu, A., Kriiska, A., Kohv, M., Hang, T., Aunap, R., 2017. GIS-based multiproxy coastline reconstruction of the eastern Gulf of Riga, Baltic Sea, during the Stone Age. *Boreas* 46, 83–99. <https://doi.org/10.1111/bor.12157>.
- Hadden, C.S., Hutchinson, I., Martindale, A., 2023. Dating marine shell: a guide for the wary north American archaeologist. *Am. Antiq.* 88 (1), 62–78. <https://doi.org/10.1017/aao.2022.82>.
- Hakonen, A., 2017. Shoreline displacement of the Finnish bothnian Bay Coast and the spatial patterns of the coastal archaeological record of 4000 BCE–500 CE. *Fennosc. Archaeol.* XXXIV, 5–31.
- Hakonen, A., 2021. Communities beyond Society: divergence of local prehistories on the bothnian arc, Northern Europe. *Open Archaeol.* 7 (1), 211–230. <https://doi.org/10.1515/opar-2020-0132>.
- Hakulinen, M., 2024. Luonnon Vatupassi – Luonoksia Järvi-Suomen Vesistöhistoriasta. Lprint Oy, Lappeenranta. ISBN 978-952-94-8789-9.
- Hedenström, A., Possnert, G., 2001. Reservoir ages in Baltic Sea sediment—a case study of an isolation sequence from the Litorina Sea stage. *Quaternary Science Reviews* 20 (18), 1779–1785.
- Herva, V.-P., Ylimaunu, T., 2014. Coastal cosmologies: long-term perspectives on the perception and understanding of dynamic coastal landscapes in the Northern Baltic Sea Region. *Time Mind* 7 (2), 183–202. <https://doi.org/10.1080/1751696X.2014.891915>.
- Herva, V.-P., Lahelma, A., 2020. Northern Archaeology and Cosmology. A Relational View. Routledge, London & New York.
- Ikonen, A.T.K., Helin, J., 2011. Development of the Olkiluoto site and implications to disposal of spent nuclear fuel. In: Ikonen, A.T.K., Lippin, T. (Eds.), *Posiva Working Report 2011-07. Olkiluoto: Posiva*.
- Jakobsson, Björck, M.S., Alm, G., Andrén, T., Lindeberg, G., Svensson, N.-O., 2007. Reconstructing the Younger Dryas ice dammed lake in the Baltic Basin: bathymetry, area and volume. *Global Planet. Change* 57 (3–4), 355–370. <https://doi.org/10.1016/j.gloplacha.2007.01.006>.
- Jöns, H., Lüth, F., Mahlstedt, S., Goldammer, J., Hartz, S., Kühn, H.-J., 2020. Germany: submerged sites in the South-Western Baltic Sea and the Wadden Sea. In: Bailey, G., Galanidou, N., Peeters, H., Jöns, H., Mennenga, M. (Eds.), *The Archaeology of Europe's Drowned Landscapes*. Springer Open, pp. 95–123.
- Jussila, T., 2000. Pioneerit Keski-Suomessa ja Savoissa. Rannansiritysmajotusmenetelmien perusteita ja vertailua. Muinaistutkija 2/2000 13–27. [http://www.sarks.fi/mt/pdf/2000\\_2.pdf](http://www.sarks.fi/mt/pdf/2000_2.pdf).
- Lahtinen, S., Jivall, L., Häkli, P., Nordman, M., 2022. Updated GNSS velocity solution in the Nordic and Baltic countries with a semi-automatic offset detection method. *GPS Solut.* 26 (9). <https://doi.org/10.1007/s10291-021-01194-z>.
- Lambeck, K., 1999. Shoreline displacement in southern-central Sweden and the evolution of the Baltic Sea since the last maximum glaciation. *Journal of the Geological Society, London* 156, 465–486.
- Lampe, R., Lampe, M., 2021. The role of sea-level changes in the evolution of coastal barriers – an example from the southwestern Baltic Sea. *Holocene* 31 (4), 515–528. <https://doi.org/10.1177/0959683620981703>.
- Lampe, R., Endtmann, E., Janke, W., Meyer, H., 2010. Relative sea-level development and isostasy along the NE German Baltic Sea coast during the past 9 ka. *E&G Quaternary Science Journal* 59 (1), 3–20. <https://doi.org/10.3285/eg.59.1-2.01>.
- Lemek, W., Jensen, J.B., Bennike, O., Endler, R., Witkowski, A., Kuijpers, A., 2002. The Darss Sill and the Ancylus Lake drainage. In: Lampe, R. (Ed.), *Holocene Evolution of the South-Western Baltic Coast – Geological, Archaeological and palaeoenvironmental Aspects*. Ernst-Moritz-Arndt University, Greifswald, pp. 175–182.
- Lidberg, M., Johansson, J.M., Scherneck, H.-G., Milne, G.A., 2010. Recent results based on continuous GPS observations of the GIA process in Fennoscandia from BIFROST. *J. Geodyn.* 50 (1), 8–18. <https://doi.org/10.1016/j.jog.2009.11.010>.
- Lindén, M., 2006. *Glaciodynamics, Deglacial Landforms and Isostatic Uplift During the Last Deglaciation of Norrbotten, Sweden*. Lund University, Lund. *PhD dissertation*.

- Lundqvist, J., 2004. Glacial history of Sweden. In: Ehlers, J., Gibbard, P.L., Hughes, P.D. (Eds.), *Quaternary Glaciations – Extent and Chronology. A Closer Look*. Elsevier B. V., pp. 401–412.
- Lunkka, J.P., 2023. The morphostratigraphic imprint of the Baltic Ice Lake drainage event in southern Finland. *Bull. Geol. Soc. Finland* 95, 47–58. <https://doi.org/10.17741/bgsf/95.1.004>.
- Lunkka, J.P., Johansson, P., Saarnisto, M., Sallasmaa, O., 2004. Glaciation of Finland. In: Ehlers, J., Gibbard, P.L., Hughes, P.D. (Eds.), *Quaternary Glaciations – Extent and Chronology. A Closer Look*. Elsevier B. V., pp. 93–100.
- Manninen, M.A., Damlien, H., Kleppe, J.I., Knutsson, K., Murashkin, A., Niemi, A.R., Rosenvinge, C.S., Persson, P., 2021. First encounters in the north: cultural diversity and gene flow in Early Mesolithic Scandinavia. *Antiquity* 95 (380), 310–328. <https://doi.org/10.15184/aqy.2020.252>.
- Meijles, E.W., Kiden, P., Streumeran, H.-J., van der Plicht, J., Vos, P.C., Gehrels, W.R., Kopp, R.E., 2018. Holocene relative mean sea-level changes in the Wadden Sea area, northern Netherlands. *J. Quat. Sci.* 33 (8), 905–923. <https://doi.org/10.1002/jqs.3068>.
- Nilsson, B., Hansson, A., Sjöström, A., 2020. Sweden: submerged landscapes of the early Mesolithic. In: Bailey, G., Galanidou, N., Peeters, H., Jóns, H., Mennenga, M. (Eds.), *The Archaeology of Europe's Drowned Landscapes*. Springer Open, pp. 77–93.
- Öhrbring, C., Petersen, G., Johnson, M.D., 2020. Glacial geomorphology between Lake Vänern and Lake Vättern, southern Sweden. *J. Maps* 16 (2), 776–789. <https://doi.org/10.1080/17445647.2020.1820386>.
- Ojala, A.E.K., Palmu, J.-P., Åberg, A., Åberg, S., Virkki, H., 2013. Development of an ancient shoreline database to reconstruct the Litorina Sea maximum extension and the highest shoreline of the Baltic Sea basin in Finland. *Bull. Geol. Soc. Finland* 85, 127–144.
- Okko, M., 1967. The relation between raised shores and present land uplift in Finland during the past 8000 years. *Ann. Acad. Sci. Fenn. Ser. A III Geol. Geogr.* 93.
- Okkonen, J., 2003. *Jäätiläisen hautoja ja hirveitä kiviröykkiöitä – Pohjanmaan muinaisten kivirakennelmien arkeologiaa*. Oulu University Press. Doctoral dissertation.
- Patton, H., Hubbard, A., Andreassen, K., Winsborrow, M., Stroeven, A.P., 2016. The build-up, configuration, and dynamical sensitivity of the Eurasian ice-sheet complex to late Weichselian climatic and oceanic forcing. *Quat. Sci. Rev.* 153, 97–121. <https://doi.org/10.1016/j.quascirev.2016.10.009>.
- Patton, H., Hubbard, A., Andreassen, K., Auricac, A., Whitehouse, P.L., Stroeven, A.P., Shackleton, C., Winsborrow, M., Heyman, J., Hall, A.M., 2017. Deglaciation of the Eurasian ice sheet complex. *Quat. Sci. Rev.* 169, 148–172. <https://doi.org/10.1016/j.quascirev.2017.05.019>.
- Påsse, T., 2001. *An Empirical Model of glacio-isostatic Movements and shore-level Displacement in Fennoscandia*. Report R-01-41. SKB, Stockholm.
- Påsse, T., Andersson, L., 2005. Shore-level displacement in Fennoscandia calculated from empirical data. *GFF* 127 (4), 253–268. <https://doi.org/10.1080/11035890501274253>.
- Påsse, T., Daniels, J., 2015. Past shore-level and sea-level displacements. *Rapporter Och Meddelanden* 137. Geological Survey of Sweden.
- Pesonen, P. E. Hertell, Mannhermaa, K., Manninen, M.A., Rostedt, T., Simponen-Robins, L., Taipale, N., Tallavaara, M., 2022. Research on the Mesolithic of North Karelia in 2003–2017. Implications for the early postglacial archaeology of Northern Europe. In: Halinen, P., Heyd, V., Mannhermaa, K. (Eds.), *Odes to Mika: Festschrift for Professor Mika Lavento on the Occasion of his 60th Birthday*, 10. Monographs of the Archaeological Society of Finland, pp. 45–55.
- Pieters, M., Missiaen, T., De Clercq, M., Demerre, I., Van Haelst, S., 2020. Belgium: prehistoric and protohistoric archaeology in the intertidal and subtidal zones of the North Sea. In: Bailey, G., Galanidou, N., Peeters, H., Jóns, H., Mennenga, M. (Eds.), *The Archaeology of Europe's Drowned Landscapes*. Springer Open, pp. 175–187.
- Quarta, G., Maruccio, L., D'Elia, M., Calcagnile, L., 2021. Radiocarbon dating of marine samples: methodological aspects, applications and case studies. *Water* 13 (7), 986. <https://doi.org/10.3390/w13070986>.
- Rosentau, A., Klemann, V., Bennike, O., Steffen, H., Wehr, J., Latinović, M., Bagge, M., Ojala, A., Berglund, M., Becher, G.P., et al., 2021. A Holocene relative sea-level database for the Baltic Sea. *Quat. Sci. Rev.* 266. <https://doi.org/10.1016/j.quascirev.2021.107071>, 107071.
- Seitsonen, O., 2005. Shoreline displacement chronology of rock paintings at Lake Saimaa, eastern Finland. Before Farming 2005/1 1–21. <https://doi.org/10.3828/bfarm.2005.1.4>.
- Sejrup, H.-P., Hjelstuen, B.O., Patton, H., Esteves, M., Winsborrow, M., Rasmussen, T.L., Andreassen, K., Hubbard, A., 2022. The role of ocean and atmospheric dynamics in the marine-based collapse of the last Eurasian Ice Sheet. *Commun. Earth Environ.* 3, 119. <https://doi.org/10.1038/s43247-022-00447-0>.
- Siiräinen, A., 1978. Archaeological shore displacement chronology in Northern Ostrobothnia, Finland. *Iskos* 2, 5–23.
- Skantsi, L., Pesonen, P., Tallavaara, M., Oinonen, M., 2023. Exception proves the rule: divergent patterns in settlement locations in Central and Southern Ostrobothnia. In: Lahelma, A., Lavento, M., Mannhermaa, K., Ahola, M., Holmqvist, E., Nordqvist, K. (Eds.), *Moving Northward, Professor Volker Heyd's Festschrift as he Turns 60*, 11. *Monographs of the Archaeological Society of Finland*, pp. 401–425.
- Smith, D.E., Harrison, S., Firth, C.R., Jordan, J.T., 2011. The early Holocene sea level rise. *Quat. Sci. Rev.* 30 (15–16), 1846–1860. <https://doi.org/10.1016/j.quascirev.2011.04.019>.
- Spratt, R.M., Lisiecki, L.E., 2016. A Late Pleistocene sea level stack. *Clim. Past* 12 (4), 1079–1092. <https://doi.org/10.5194/cp-12-1079-2016>.
- Stattegger, K., Leszczyńska, K., 2023. Rapid sea-level rise during the first phase of the Litorina transgression in the western Baltic Sea. *Oceanologia* 65 (1), 202–210. <https://doi.org/10.1016/j.oceano.2022.05.001>.
- Steffen, H., Wu, P., 2011. Glacial isostatic adjustment in Fennoscandia—A review of data and modeling. *J. Geodyn.* 52, 169–204. <https://doi.org/10.1016/j.jog.2011.03.002>.
- Stroeven, A.P., Hästeström, C., Kleman, J., Heyman, J., Fabel, D., Fredin, O., Goodfellow, B.W., Harbor, J.M., Jansen, J.D., Olsen, L., Caffee, M.W., Fink, D., Lundqvist, J., Rosqvist, G.C., Strömbärg, B., Jansson, K.N., 2016. Deglaciation of fennoscandia. *Quat. Sci. Rev.* 147, 91–121. <https://doi.org/10.1016/j.quascirev.2015.09.016>.
- Tallavaara, M., Pesonen, P., 2020. Human ecodynamics in the north-west coast of Finland 10,000–2000 years ago. *Quat. Int.* 549, 26–35. <https://doi.org/10.1016/j.quaint.2018.06.032>.
- Tikkanen, M., Oksanen, J., 2002. Late Weichselian and Holocene shore displacement history of the Baltic Sea in Finland. *Fennia* 180 (1–2), 9–20.
- Uścinowicz, S., 2004. Rapid Sea Level Changes in the Southern Baltic During Late Glacial and Early Holocene, 11. Polish Geological Institute Special Papers, pp. 9–18.
- Vaneekhout, S., 2009. Aggregation and polarization in northwest coastal Finland : socio-ecological evolution between 6500 and 4000 cal BP. Doctoral dissertation. Oulu: University of Oulu.
- Vaneekhout, S., Okkonen, J., Costopoulos, A., 2012. Paleoshorelines and prehistory on the eastern Bothnian Bay coast (Finland): local environmental variability as a trigger for social change. *Polar Geogr.* 35 (1), 51–63.
- Vestøl, O., Ågren, J., Steffen, H., Kierulf, H., Tarasov, L., 2019. NKG2016LU: a new land uplift model for Fennoscandia and the Baltic Region. *J. Geod.* 93, 1759–1779. <https://doi.org/10.1007/s00190-019-01280-8>.
- Vuorela, A., Penttilä, T., Lahdenperä, A.-M., 2009. Review of Bothnian Sea shore-level displacement data and use of a GIS tool to estimate isostatic uplift. *Posiva Working Report 2009-17*. Posiva Oy, Olkiluoto.
- Žulkus, V., Girininkas, A., 2022. Changes in Baltic Sea relict coasts and the subsistence economy in Lithuania in the late Pleistocene and early Holocene. In: Girininkas, A., Žulkus, V. (Eds.), *Lithuanian Baltic Sea Coasts During the Holocene*. BAR Publishing, Oxford, pp. 15–40. <https://doi.org/10.30861/9781407359878>.